Electrical Characterization of Concrete Using the Parallel Plate Capacitor Method

Marcelo B. Perotoni [1], Marcos S. Vieira [2], Kenedy M. dos Santos [3], and Danilo B. Almeida [3]

[1] UFABC
Santo Andre, SP,09210-580, Brazil
Marcelo.perotoni@ufabc.edu.br

[2] Mackenzie Presbyterian University
Sao Paulo, SP, 01302-907, Brazil
marcos.vieira@mackenzie.br

[3] IFBA
Vitoria da Conquista, BA, 45078-900, Brazil
kenedymarconi@gmail.com

Abstract — This article describes the measurement of the complex dielectric constant of pure concrete and a brick wall, in the frequency range up to 2 MHz, with a view towards more accurate material description in electromagnetic simulations. The measurement system is based on the use of the materials under test as the dielectric material placed inside a parallel plate capacitor, in series with an external known fixed resistor. The theory behind the measurement is covered, and the results of both real and imaginary relative dielectric constants for both materials are presented. Finally, an electromagnetic simulation showing the shielding effectiveness of a hollow box made of a brick wall is presented, using the measured data in comparison with data from a commercial simulator database.

Index Terms — Electromagnetic compatibility, materials testing, numerical simulation, shielding.

I. INTRODUCTION

The importance of correctly addressing the lightning effect on buildings and structures increases with the number of sensitive electronic systems inside [1-3]. Real world tests of lightning strikes on buildings and structures are complicated, therefore computer simulations are attractive, and permit evaluation of a first order effect of the induced fields inside. Lightning simulators that generate equivalent currents and resultant electromagnetic field waveforms are still large and complex. Existing regulations and literature present some analytical waveforms that represent typical lightning strikes. Correct material characterization ensures more reliable computer simulations. Not only lightning studies benefit from the correct material description, also applications where the electromagnetic shielding of a room or closed area is important, such as when dealing with secure communications, resistant against Tempest (NATO and NSA - National Security Agency given name for spying activities based on unintended electromagnetic emissions) or other similar eavesdrop methods [4, 5]. Walls made of reinforced concrete with an internal metallic frame could help isolate and contain the major part of the fields outside the volume, preventing undesired field configuration inside the structure based on unintended emissions.

Several papers cover the measurement of the electrical permittivity of concrete. However, most of these studies aim to electrically characterize the concrete in the range of the microwave and RF frequencies, from a few hundred to a few thousand Megahertz.

The reflection and transmission of a CW (Continuous Wave) signal incident on a concrete block are used to compute the material complex dielectric constant [6]. A cylindrical coaxial transmission line was built using concrete poles as the dielectric core, whose water content was varied and used to measure the complex dielectric constant from 50 MHz to 1.6 GHz using two different methods [7]. Other technique measured several materials used in construction by fitting measured time domain reflection and transmission signals to the Kirkwood-Fuoss equation, the measured data obtained from two antennas connected to a vector network analyzer (frequency range from 1 GHz to 6 GHz), with the sample material as an obstacle [8]. GPR (Ground Penetration Radar) has been used to address material parameters measurements, such as asphalt, for frequencies between 900 MHz and 1.5 GHz [9] and also concrete, for frequencies on the range of 500 MHz and 5 GHz [10]. Time-Domain Reflectometry (TDR) was also employed

Submitted On: April 10, 2019
Accepted On: May 7, 2019

to determine the electrical parameter of concrete, in the range of 100 MHz to 1 GHz [11]. Measurements of complex dielectric constants at lower frequencies employ the step voltage [12, 13] with variants of Wheatstone bridges in capacitors built with guard electrodes, as to diminish fringing fields.

Since most of the studies focus on the VHF and UHF range, to address losses associated with indoor wireless communication, this work presents a simple and low-cost method based in a material-filled parallel plate capacitor, focusing on frequencies that are present in lightning strikes and other emission and susceptibility analyses, up to 2 MHz. The instrumentation is based on a signal generator, oscilloscope and the test capacitor is built considering the characteristics and size of the concrete material.

II. MEASUREMENT THEORY

In the electrical model presented in Fig. 1 the external reference resistor *R* is placed in series with the capacitor, symbolized by the lumped element *C* and its loss resistor R_L, also known as the capacitor Equivalent Series Resistance, or ESR. The loss resistor is considered to be in series in cases where the leakage current is low, other than that it is presented as a shunt element [12]. It is worth mentioning that the ESR value typically varies with frequency [14]. From the capacitor *C* it is possible to extract the real value of the permittivity (ε') whereas the loss resistor will relate to the imaginary part (ε''). V_1 and V_2 are the nodes whose voltages are measured, using two channels of the oscilloscope. Since the two elements that represent the capacitor cannot be accessed individually, the two physical quantities need to be indirectly found.

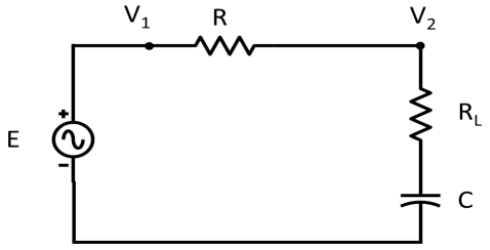

Fig. 1. Electric model representing the measurement system.

Figure 2 shows the quantities effectively measured with the oscilloscope, with a bold trace: the voltages V_1 and V_2 and their respective phase. Since the real and imaginary parts that model the capacitor cannot be physically separated, indirect manipulations will eventually provide their results.

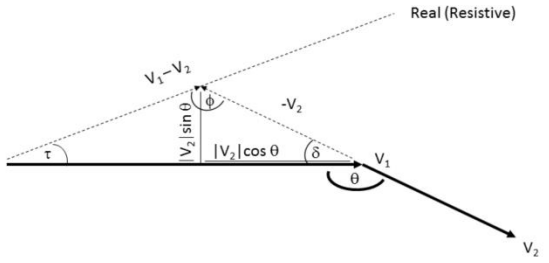

Fig. 2. Phasor representation of the measured quantities.

From Fig. 2 the vector subtraction between both measured voltages is the voltage drop on the external resistor *R* - therefore it is purely real. The current in the series circuit is found to be:

$$I = \frac{\sqrt{V_1^2+V_2^2-2V_1V_2\cos\theta}}{R}. \quad (1)$$

The numerator expresses the voltage drop on the external resistor (using the law of cosines). The complex impedance of the capacitor is given by:

$$Z_C = R_L + \frac{1}{j\omega C} = \frac{V_2 R}{\sqrt{V_1^2+V_2^2-2V_1V_2\cos\theta}}. \quad (2)$$

The angle ϕ, once found, will permit describe both real (the R_L voltage drop) and imaginary (due to *C*) voltages in terms of the three measured quantities. The following relation is valid for the internal angles of the triangle:

$$\phi + \delta + \tau = \pi, \quad (3)$$

δ, however, is equal to $(\pi - \theta)$. Therefore, the angle ϕ can be written as:

$$\phi = \theta - \tau. \quad (4)$$

The angle τ can be written as:

$$\tau = \operatorname{atan}\left(\frac{|V_2|\sin\theta}{|V_1|-|V_2|\cos\theta}\right), \quad (5)$$

so that it provides:

$$\phi = \theta - \operatorname{atan}\left(\frac{|V_2|\sin\theta}{|V_1|-|V_2|\cos\theta}\right). \quad (6)$$

Figure 3 shows again the real and imaginary phasors of V_2. It is possible then to isolate both real and imaginary parts of the capacitor voltage.

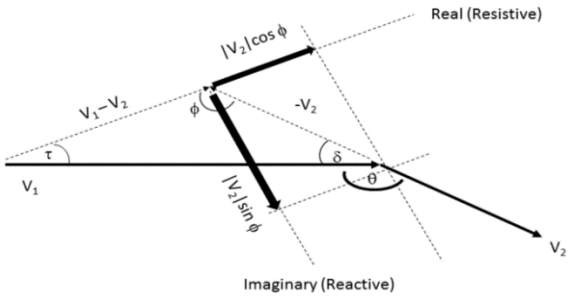

Fig. 3. Decomposition to extract the V2 components.

Using (2) and (6), the complete capacitor model can be written as:

$$Z_C = R_L + \frac{1}{j\omega C} = Z_C(\cos\phi - j.\sin\phi). \quad (7)$$

Neglecting the fringing fields of the parallel plate capacitor, the real part of the permittivity can be found using (8), where d is the distance between both plates; A indicates their respective area and ε_o the absolute (vacuum) permittivity:

$$\varepsilon_r' = \frac{Cd}{A\varepsilon_o}. \quad (8)$$

Considering the loss tangent (*tan D*) definition as in (9):

$$\tan D = \frac{\varepsilon''}{\varepsilon'} = \frac{R_L}{|X_C|}. \quad (9)$$

The imaginary part of the permittivity is then found after the relation from (10), with ω representing the angular frequency (recalling that R_L physically represents the ESR):

$$\varepsilon'' = R_L \omega C \varepsilon'. \quad (10)$$

The measurement setup needs a signal generator and oscilloscope, with at least two channels. The generator sets the signal frequency of a sinusoidal wave with adequate amplitude, and both oscilloscope channels inform the voltage amplitudes and their phase difference, in degrees.

III. MEASUREMENT RESULTS: SOLID CONCRETE

A parallel plate capacitor, square (length of 30 cm) is filled with concrete (3 cm thick) according to Fig. 4. For this specific case, the mixture is pure concrete (water, cement, and sand as aggregate, in equal proportions), i.e., there are no further elements such as rocks or steel.

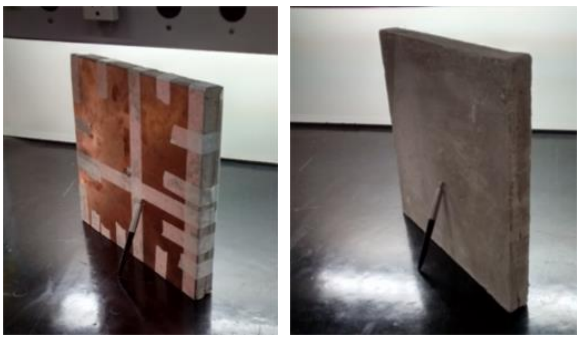

Fig. 4. (Left) Capacitor with its metallic plates and (right) its dielectric inner part.

Two sets of measurements were performed: one with a fresh concrete (3 days old) and other one cured or dried (3 months old). Results are presented in Fig. 5 and also in Table 1.

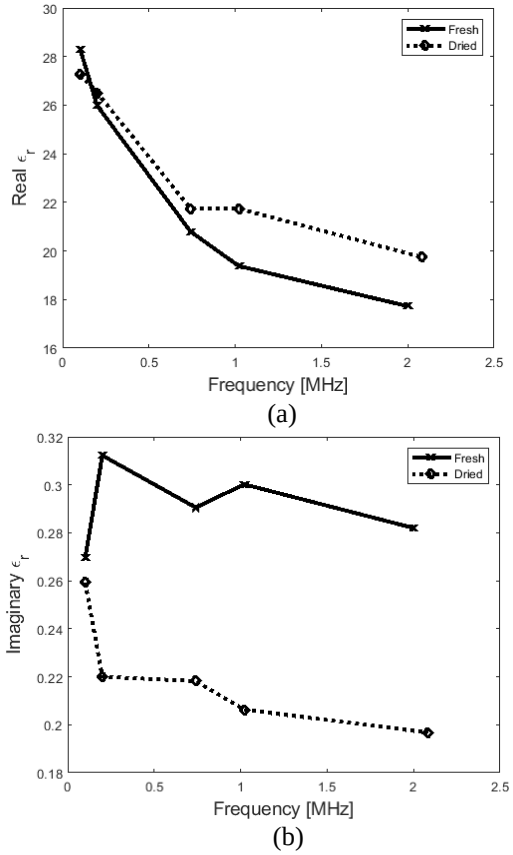

Fig. 5. Measured: (a) εr' and (b) εr'' for pure concrete.

Table 1: Measured relative dielectric constant

	Fresh		Dry	
Frequency [MHz]	**ε_r'**	**ε_r''**	**ε_r'**	**ε_r''**
0.10	28.31	0.26	27.27	0.26
0.20	25.97	0.31	26.50	0.22
0.74	20.79	0.29	21.74	0.21
1.02	19.38	0.30	21.74	0.20
2.00	17.72	0.28	19.74	0.20

During the measurements, as the frequency was swept, the external resistor R was set (using a potentiometer) so that the voltage drops on V_1 and V_2 were kept constant (for this case, with a ratio $V_1/V_2 \approx 1.67$). The results showed that the dry concrete has a slightly higher ε_r' in comparison to the fresh – where the water content is still high. As for the losses, the fresh concrete showed that ε_r'' was higher than the dried material, indicating the water again as the likely responsible for the observed higher dielectric losses. A similar study, for the frequencies 500 MHz and covering the 1 GHz to 2 GHz also showed a substantial variation on the complex permittivity due to the moisture content [15].

IV MEASUREMENT RESULTS: SOLID CONCRETE

A real masonry wall was built, with dimensions of 1.4 x 1.6 x 0.16 meters. It employed concrete bricks (shown in Fig. 6) and was covered with a cement mixture layer, as to emulate real walls. It was covered with a thin aluminum metallic sheet- to work as the contact plates. The measurement workflow followed suit the presented in the former section, but for safety reasons, the concrete cure time was duly observed, so only the dry condition was evaluated.

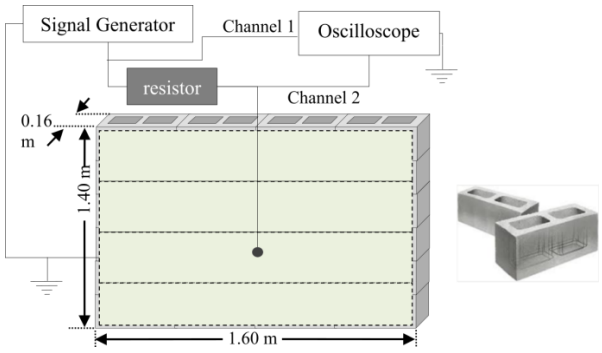

Fig. 6. (Left) real masonry wall used for concrete permittivity characterization and (right) concrete block used.

Table 2 provides the permittivity (real and imaginary) results and Fig. 7 shows the respective plots.

Table 2: Measured relative dielectric constant

Frequency [MHz]	ε_r'	ε_r''
0.05	32.89	0.29
0.10	27.67	0.25
0.15	19.19	0.25
0.20	19.07	0.37
0.25	17.25	0.44
0.30	16.22	0.45
0.35	15.59	0.43
0.40	14.45	0.51
0.50	12.95	0.58
0.75	10.48	0.48
1.00	9.16	0.51
1.21	8.96	0.50
1.50	8.24	0.46
1.70	8.15	0.48
2.00	7.95	0.48
2.30	7.60	0.45

It can be seen that the wall has smaller values for εr' in comparison to the pure concrete, given to the fact there is a larger air content on bricks not totally solid.

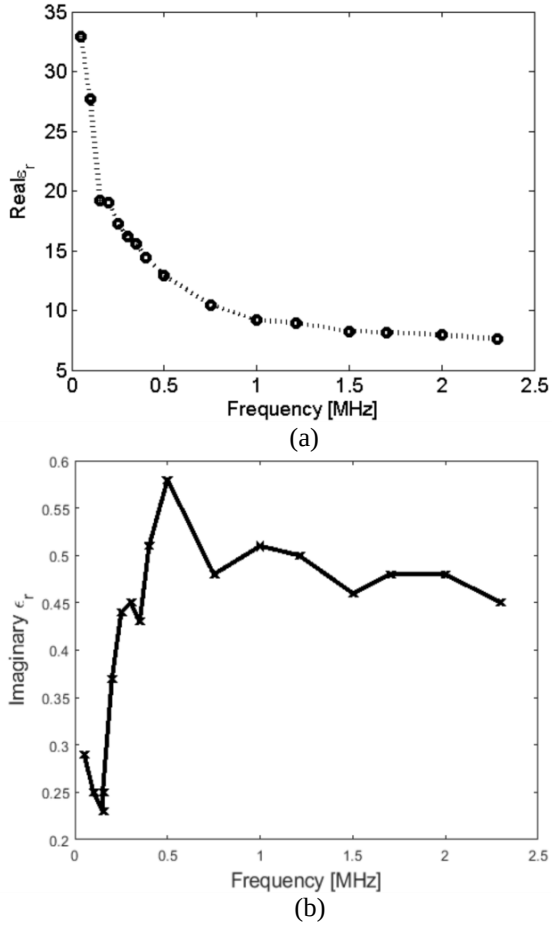

Fig. 7. Measured: (a) εr' and (b) εr'' for the wall.

V. APPLICATION: SHIELDING SIMULATION

With the proper material data, one is able to more accurately address electromagnetic effects in simulation tools. To exemplify it, the electromagnetic shielding provided by a brick box (according to Table 2) is simulated, against an incident plane wave (Fig. 8). The simulation was performed within FEKO, based on the Method of Moments (MoM) [16]. The MoM discretizes the structure in a tetrahedral mesh so that the integral equation is solved in an iterative way. The matrix is usually ill-conditioned, and to speed up the solution an MLFMM (Multi-Level Fast Multipole Method) can be employed, where the coupling among distant elements is considered zero [17]. For this specific problem, the pure MoM method was used since it is not electrically large. The plane wave has a broadband spectrum, covering DC to 2.3 MHz, amplitude of 1 V/m. The simulation model has a simple box with 4m length and wall thicknesses of 16 cm.

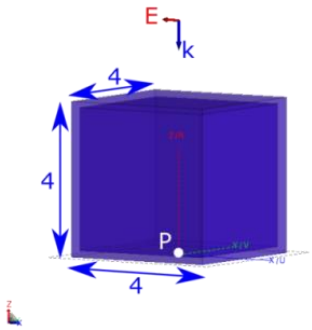

Fig. 8. Model used for the simulation. The plane wave is shown at top.

The electric field is measured by a probe (marked *P* in Fig. 8) placed on the bottom of the box volume. Figure 9 shows the comparison between the electric field attenuation (i.e., comparing the electric field amplitude on the point P for the free space and concrete box scenarios) inside the box with its material description given by the measurements (Table 2) and the available material data for "Construction Brick", inside FEKO database. The material data corresponds to the higher frequencies, starting from 1 GHz, and the lower range of frequencies is obtained after interpolation. It can be seen that the attenuation using the electrical material characteristics from the measurements resulted in a much larger attenuation across a large part of the frequency range.

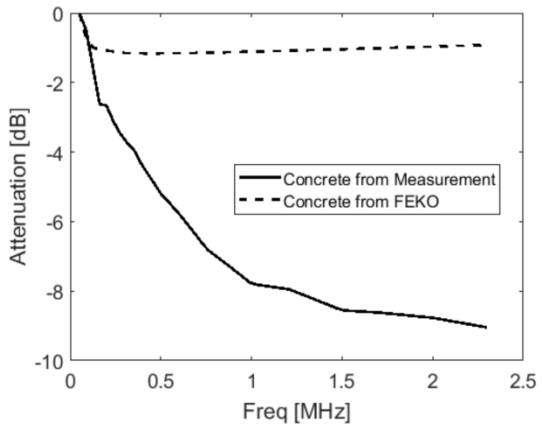

Fig. 9. Computed attenuation of the Electric Field inside the box, for two types of concrete.

VI. CONCLUSION

The article covered a simple and low-cost method to measure the electrical characteristics of concrete, which was applied to either a small block and also to a large wall. The results provided the material characterization in a frequency range where available similar results were not found by the authors, and whose importance is vital for applications in lower frequencies (down to few MHz), like lightning strikes and electromagnetic shielding. Comparison to existing data inside the material database of commercial numerical field codes also shown that the attenuation considering the measured material is larger, across the almost entire band up to 2.5 MHz.

REFERENCES

[1] J. Kato, H. Kawano, T. Tominaga, and S. Kuramoto, "Investigation of lightning surge current induced in reinforced concrete buildings by direct strikes," *2001 IEEE International Symposium on Electromagnetic Compatibility*, pp. 1009-1014, 2001.

[2] J. Chen, B. Zhou, F. Zhao, and S. Qiu, "Finite-difference time-domain analysis of the electro-magnetic environment in a reinforced concrete structure when struck by lightning," *IEEE Transactions on Electromagnetic Compatibility*, vol. 52, no. 4, pp. 914-920, Nov. 2010.

[3] IEEE 299-2006 - *IEEE Standard Method for Measuring the Effectiveness of Electromagnetic Shielding Enclosure*, 2006.

[4] S. Pennesi and S. Sebastiani, "Information security and emissions control," *2005 IEEE International Symposium on Electromagnetic Compatibility*, pp. 777-781, 2005.

[5] H. Seikiguchi and S. Seto, "Study on maximum receivable distance for radiated emission of information technology equipment causing information leakage," *IEEE Transactions on Electromagnetic Compatibility*, vol. 55, no. 3, pp. 547-554, June 2003.

[6] X. Hui, L. Bangyu, X. Shaobo, and F. Hongzhuan, "The measurement of dielectric constant of the concrete using single-frequency CW radar," *First International Conference on Intelligent Networks and Intelligent Systems*, pp. 588-591, 2008.

[7] G. Villain, A. Ihamouten, and X. Dérobert, "Use of frequency power law to link the results of two testing methods for the characterization of humid concretes," *2011 6th International Workshop on Advanced Ground Penetration Radar (IWAGPR)*, pp. 1-5, 2011.

[8] C. A. Grosvenor, R. T. Johnk, J. Barker-Jarvis, M. D. Janezic, and B. Riddle, "Time-domain free-field measurements of the relative permittivity of building materials," *IEEE Transactions on Instrumentation and Measurements*, vol. 58, no. 7, pp. 2275-2282, July 2009.

[9] S. Ji-tong, G. Xiu-jun, Z. Xiao-wei, "Research on dielectric properties of asphalt concrete with GPR," *2012 14th International Conference on Ground Penetration Radar (GPR*), pp. 542-545, 2012.

[10] Z. Yanhui, Z. Bei, S. Wenbo, and W. Tao, "Experimental research on relationships between dielectric constant of cement concrete materials

and measuring frequency," *2012 14th International Conference on Ground Penetrating Radar (GPR)*, pp. 403-406, 2012.

[11] S. Lihua, X. Qiwei, C. Bin, and G. Cheng, "Measurement of the frequency-dependent dielectric constant of concrete materials by TDR and wavelet modeling method," *CEEM 2003 Asia-Pacific Conference on Environmental Electromagnetics*, pp. 626-629, 2003.

[12] J. G. Webster, *The Measurement, Instrumentation and Sensors Handbook (Electrical Engineering Handbook)*. CRC Press, pp. 1402-1413, 1998.

[13] A. V. Hippel, *Dielectric Materials and Applications*. MIT Technology Press and John Wiley & Sons, pp. 47-63, 1954.

[14] S. Pfeifer, S. H. Park, and P. R. Bandary, "Modeling the relative dielectric permittivity and impedance of carbon nanotube constituted polymer composites in the sub-GHz regime," *ECS Solid State Letters*, vol. 2, no. 1, pp. M5-M7, Oct. 2012.

[15] X. Jin and M. Ali, "Simple empirical formulas to estimate the dielectric constant and conductivity of concrete," *Microwave and Optical Technology Letters*, vol. 61, no. 2, pp. 386-390, Feb. 2019.

[16] M. N. O. Sadiku, *Numerical Techniques in Electromagnetics*. CRC Press, pp. 274-336, 2001.

[17] J. J. von Tonder and U. Jakobs, "Fast multipole solution of metallic and dielectric scattering problems in FEKO," *IEEE/ACES International Conference on Wireless Communications and Applied Computational Electromagnetics, 2005.*

Marcelo B. Perotoni Electrical Engineer (UFRGS, Porto Alegre, Brazil), M.Sc. and Ph.D. in Electrical Engineering from USP (Sao Paulo, Brazil). He has been involved with electromagnetic simulation since 2002 and is interested in RF and EMC. He is currently a professor at UFABC.

Marcos S. Vieira B.Sc. in Electrical Engineering (1996) - UMC, M.Sc. in Electrical Engineering (2004) - Mackenzie Presbyterian University, Ph.D. in Electrical Engineering (2015) - USP (Sao Paulo, Brazil). Currently is a Professor at the Mackenzie Presbyterian University. He has experience in Electrical Engineering with emphasis on Numerical Methods, Microwave and Antennas.

Kenedy M. G. Santos is B.Sc. in Electrical Engineering (2006) - PUC MG, M.Sc. in Electrical Engineering (2011)-UFMG, Ph.D. in Electrical Engineering (2018) - UFBA. Currently is Professor at the IFBA. He has experience in Electrical Engineering with emphasis on EMC, Microwave and Antennas.

Danilo B. Almeida is B.Sc. in Electrical Engineering (2005) - UNIP - SP. He is a specialist in Occupational Safety and Energy Efficiency. Currently is Professor at the IFBA and FAINOR.